

Mars Technology Program (MTP) Communications and Tracking Technologies for Mars Exploration^{1,2}

Dimitrios Antsos
818-354-6343

Dimitrios.Antsos@jpl.nasa.gov

Jet Propulsion Laboratory
California Institute of Technology
4800 Oak Grove Drive
Pasadena, CA 91109

Abstract—The future of the exploration of Mars will see an unprecedented increase in the volume of data generated by an increasingly capable host of science instruments on various rovers, aerobots, orbiters and eventually humans on Mars. To return these large volumes of data to Earth communication links with data-rate capabilities in the multiple megabits-per-second will be required. The MTP of the National Aeronautics and Space Administration (NASA), managed by the Jet Propulsion Laboratory (JPL) of the California Institute of Technology, has invested in a technology development portfolio, the Communications and Tracking Technology Development Program, the aim of which is to develop critical enabling technology components and products that will make these future high-capacity communications links from Mars possible.

The MTP Communications and Tracking Technology Development Program comprises the following ten technology development tasks:

- (1) Reprogrammable Transceiver Modem for the Electra Radio.
- (2) Mars Proximity Microtransceiver.
- (3) X-Band Appliqué for the Electra Radio.
- (4) X-Band Agile Beam Transmitter.
- (5) Combined UHF/X-Band Proximity Link Antennas.
- (6) Large Fresnel Lenses for Optical Ground Receivers.
- (7) Coding System for High Data-Rate Mars Links.
- (8) Fast and Accurate Electromagnetic (EM) Modeling.
- (9) Adaptive Data-Rates for Electra.
- (10) Autonomous Radios for Proximity Links.

In this paper we briefly describe each task and give a summary of the current state of the research and future recommendations.

TABLE OF CONTENTS

1. INTRODUCTION.....	1
2. THE CURRENT CAPABILITY.....	1
3. OPPORTUNITIES FOR FUTURE IMPROVEMENT.....	3
4. DESCRIPTION OF THE TASKS.....	4
5. ACKNOWLEDGMENTS.....	18
REFERENCES.....	19
BIOGRAPHIES.....	19

1. INTRODUCTION

The Mars Exploration Program (MEP) of NASA, run by JPL, is planning a host of exploration spacecraft that will visit Mars in the future, on the average one every two years.

These spacecraft will carry increasingly capable scientific instruments, which will produce more and more data. The MTP of the MEP has recognized the need for advances in the communications and tracking technologies, so that the lack of capability of the data pipeline from Mars to Earth does not limit the set of possible missions. The MTP has competitively selected and funded a technology development portfolio aiming to advance the current state of the art in communications and tracking technologies and infuse the outputs of this research to future Mars and other Mars Missions.

2. THE CURRENT CAPABILITY

There are currently two NASA spacecraft in Mars orbit capable of relaying data from other spacecraft to Earth: the Mars Global Surveyor (MGS) and Mars Odyssey [1]. The telecommunications relay radio on MGS is a Frequency-Shift Keying (FSK) Ultra-High Frequency (UHF) radio, named Mars Relay that was built by the Centre National d'Etudes Spatiales (CNES), the French space agency. It supports a maximum return link (from the surface of Mars to the orbiter) data rate of 128 kbps. The telecommunications relay radio on Mars Odyssey is the Command/Telemetry Transceiver (C/TT) 505 built by CMC

¹ 0-7803-9546-8/06/\$20.00© 2006 IEEE

² IEEEAC paper #1247, Version 4, Updated November 11, 2005

Electronics Cincinnati (now L-3 Communications Cincinnati Electronics). It supports a maximum return link data rate of 256 kbps using coherent Phase-Shift Keying (PSK) modulation and convolutional/Viterbi encoding/decoding.

The two Mars Exploration Rovers (MERs), named Spirit and Opportunity, which were launched a few weeks apart in the summer of 2003, have been exploring Mars since their successful landing and deployment in January 2004. These rovers each have two communications systems on board: an X-Band (7.2 GHz uplink, 8.45 GHz downlink) communications system, for Direct-To-Earth (DTE) communication, and a C/TT 505 UHF radio, for communication with MGS and Odyssey over the UHF "proximity link."

Almost 90% of the data returned by the two rovers has been communicated over the Mars Odyssey UHF proximity link and relayed back to Earth over X-Band. The rovers' UHF proximity link has been heavily favored because it is 22 times more energy efficient than their DTE link: whereas the DC power consumption of the two rover communications systems is comparable (45 Watts of the UHF versus 70 Watts of the X-Band), the achievable data rate of the UHF link (256 kbps) is more than an order of magnitude greater than that of the X-Band link (up to 18 kbps when the distance between Mars and the Earth is 1.1 Astronomical Units (AU)). Mars Odyssey has been the relay orbiter of choice because it supports a higher data rate than MGS (256 kbps versus 128 kbps), has a larger onboard storage capability than MGS (32 MB versus 9.6 MB), and provides more error-free data than MGS, due to its use of the Proximity-1 Space Link protocol [2].

Mars Odyssey is in a circular, polar, and sun-synchronous orbit of 400 km altitude with a period of approximately 2 hours. The MER rovers are on opposite sides of Mars, near the equator. This results in 2 or 3 orbits per sol (a Martian day, approximately 24 hours and 40 minutes long) with passes suitable for communicating with the rovers. The duration of Odyssey's passes, from the rovers' point of view, is between 12 and 15 minutes, from 5-degree elevation to 5-degree elevation. Therefore, the theoretical maximum data return per day from a rover is 3 passes/day x 15 minutes per pass x 60 seconds per minute x 256 kbps = 675 Mbits = 84.4 MB. This assumes that the maximum 256 kbps data rate can be sustained throughout all 3 usable passes of a given sol. In a more typical scenario, where only 128 kbps can be maintained over the link, only 2 usable Odyssey passes occur, and the passes are 13.5 minutes long 172 Mbits (21.5 MB) can be returned by one rover in a single day [2].

An average data return of 172 Mbits per day, impressive as it is considering the data is coming from Mars, will be inadequate to cover the future needs of various planned missions, which may include balloons, gliders, airplanes,

penetrators and landers, equipped with increasingly capable instruments that will return a lot of data. Even the panoramic cameras on the MERs generate full panoramic pictures of 10 Gbits uncompressed size (400 Mbits with lossy compression).

To support the increasing telecommunications demands of the future of Mars exploration, NASA has developed a new advanced radio, the Electra Proximity Link Payload, which can support much higher data rates than the 256 kbps of the C/TT 505, and can provide full duplex "transponding" with coherent Doppler turnaround, to assist in precise navigation and position determination [3].

The first spacecraft carrying the Electra radio was the Mars Reconnaissance Orbiter (MRO), which launched in August 2005. The Electra radio is a fully reconfigurable, frequency-agile transceiver. The core of the Electra radio, and the reason for its flexibility and reconfigurability, is its Baseband Processor Module (BPM), a flight-programmable electronics module, which offers digitally implemented modulation and demodulation functions, provides standardized link layer protocols, manages interfaces with the spacecraft, and implements overall payload control. The BPM incorporates two key reconfigurable elements: a Payload Controller, based on a SPARC 32-bit microprocessor, and a Modem Processor (MP) utilizing a 1 MGate Xilinx reprogrammable Field Programmable Gate Array (FPGA).

Some key specifications of the Electra radio are [3]:

- Data Rates (with rate ½ convolutional code):
 - 0.5, 1, 2, 4, 8, 16, 32, 64, 128, 256, 512, 1024 kbps
- Frequencies (on-orbit tunable in 56 kHz steps):
 - Full Duplex RX: 390 to 405 MHz
 - Full Duplex TX: 435 to 450 MHz
 - Half Duplex RX and TX: 390 to 450 MHz
- Modulations:
 - Manchester and NRZ-L Binary Phase Shift Keying (BPSK)
 - 60° and 90° Modulation Index.
- Channel Coding:
 - Reed Solomon
 - K=7, R=1/2 Convolutional Code/Decode
- Receiver Noise Figure:
 - Full Duplex: 4.9 dB
 - Half Duplex: 3.9 dB
- Receive Signal Dynamic Range: -140 dBm to -70 dBm
- Transmit Power:
 - Full Duplex: 5 W
 - Half Duplex: 7 W
- Protocols: CCSDS Proximity-1 compliant
- Mass: 5.0 kg (with diplexer)
- Volume: 5080 cm³

Since Electra is a “software radio,” many other modulation waveforms and modes operation, far beyond those listed above, are realizable.

3. OPPORTUNITIES FOR FUTURE IMPROVEMENT

Our objective in the Communications and Tracking element of the MTP is to increase the aggregate quantity of data that can be transmitted from Mars to the Earth. Fixing the landing locations and orbits of the different spacecraft (explorers and relay orbiters) with respect to each other and to the Earth, fixes the time windows of relative visibility (or “passes”) between different spacecraft and the Earth, hence the communications periods (since we need line-of-sight to communicate). Therefore, to increase the aggregate data return, we ultimately have to increase the data rate of communication.

The achievable data rate of a communications link is proportional to the power of the electromagnetic wave received by the receiver. This received power is related to other link parameters, such as antenna size and communications distance by the *Friis Free-Space Transmission Formula*, which can take four different forms:

$$P_R = \frac{A_R A_T}{c^2 L^2} \cdot f^2 \cdot P_T \quad (1)$$

$$P_R = G_R \left(\frac{c}{4\pi fL} \right)^2 G_T P_T \quad (2)$$

$$P_R = A_R \frac{G_T P_T}{4\pi L^2} = \frac{G_R}{4\pi L^2} A_T P_T \quad (3)$$

where P_T and P_R are the transmitted and received powers, respectively, A_T and A_R are the effective areas of the transmitting and receiving antennas, G_T and G_R are the gains of the transmitting and receiving antennas, L is the distance between the transmitter and the receiver (sometimes referred to as the communications range), f is the communications frequency, and c is the speed of light. The effective area of an antenna is the area of a uniformly illuminated disk that produces the same power density at the same spot in the far-field (far enough that the wavefronts are plane), in a direction perpendicular to the disk, as the antenna does in the direction of its maximum radiation, when both the disk and our antenna are fed by an equal power electromagnetic wave. The gain of an antenna is the ratio of the power density it produces in the far-field to the power density an isotropic radiator would produce at the same spot, when fed by an equal power electromagnetic wave.

Equations (1) – (3) are very instructive in ways that we can increase the received power (hence the data rate). An obvious way is to increase the transmitted power, P_T . We can do this by increasing the output power of the power amplifier that is connected to the antenna. A higher output power, however, translates to a higher DC power consumption, and power is a scarce resource on some of the scout-class surface landers described above. *If* we can increase the amplifier output power *without* increasing its DC power consumption, i.e. if we can simultaneously increase its output power *and* its efficiency, then we can improve the communications link with no system “penalty.”

Another way to increase the received power is to increase the effective area or gain of the communications antennas. Antennas in general fall into two general categories: low gain (broad beam, low directivity) antennas and high (or medium) gain antennas. Examples of low gain antennas are monopoles, dipoles, drooping dipoles, microstrip patches, and quadrifilar helical antennas. The operation of these antennas depends on a single or a combination of resonant elements that radiate to produce a very broad beam, sending radiation towards most of the 2π steradians of a half-space. High gain antennas are based on paraboloid reflectors, which produce a plane in-phase wave at infinity from power emanated by a point source at their focus. High gain antennas focus the electromagnetic radiation into a relatively narrow beam (a few degrees or less), thereby increasing the power of the received wave.

Currently both the Mars Odyssey orbiter and the MERs carry low gain antennas (a quadrifilar helix and a quarter-wave monopole, respectively). This is so that Mars Odyssey can communicate with each MER regardless of the relative attitude of the two spacecraft, which changes as Odyssey orbits Mars, and the rovers drive around. Using medium or high gain antennas instead would increase the received power, but the radiation beam of the antenna would have to be steered to maintain line-of-sight communication as the geometry of the link changes with relative motion. There are two methods of antenna beam steering: mechanically, by steering the whole antenna with gimbals, and electronically, by changing the phase across a radiating aperture. Gimbals add to the mass, volume and power of the spacecraft, while reducing reliability. Electronic steering, depending on the specific implementation, may also impact some of the above parameters, although it can also have distinct advantages over mechanical steering (e.g. graceful degradation, and faster steering rates).

Another related parameter of equations (1)-(3) we can vary to increase the received power is the communications frequency. In the future an X-Band module will be made available, as an option, for the Electra radio. As we see from equations (1)-(3), however, increasing the communications frequency is only beneficial if both communicators use high directivity, high gain (i.e.

steerable) antennas (equation (1)). In that case, the received power increases proportionally to the square of the ratio of the frequencies. Therefore, assuming high gain, steerable antennas on both spacecraft, the received power at the orbiter would increase by a factor of $(8415 \text{ MHz}/401.5 \text{ MHz})^2 = 440$ or 26.4 dB. If one spacecraft only uses a steerable, high gain antenna (and assuming its size is the same for both frequencies) and the other a low gain, broad beam antenna, then we neither gain nor lose by going up in frequency (equation (3)). Finally, if both spacecraft have low gain antennas on board, the received power *decreases* with the square of the communications frequency (equation (2)).

There are other ways of increasing the received data volume, without increasing the data rate. One such way is by improved coding. By mapping raw communications bits into special code symbols, which are actually broadcast over the communications channel, we can communicate with less bit energy (i.e. higher data rate) for a given bit error rate. There is an ultimate upper limit in the data rate at which we can communicate over a given channel at a given bit error rate. This limit is called the channel capacity or the Shannon limit. The performance of a combination of Reed-Solomon and convolutional coding, currently used in both the C/TT 505 transceiver and the Electra radio, is 2.5 to 3 dB away from the channel capacity (the theoretical maximum). Recent advances in coding have resulted in the development of so called Low Density Parity Check (LDPC) codes. These codes perform about 2 dB better than Reed Solomon/convolutional codes, thus reducing the gap from channel capacity to only 0.5 to 1 dB, and resulting in increased data rates (2 dB translates to a factor of 1.6) for the same received carrier power.

Another way to increase the received data volume is by eliminating link margin. Link margin refers to the fact that we set the data rate of a communications session between a lander and an orbiter a priori, based on predictions of the received power at the orbiter, based on the radiation patterns of the two antennas, and the relative geometry of the pass. When we set this data rate we do so conservatively, often with many dB of margin, and set it low enough to allow for communication at the worst points of the pass, where the received carrier power at the orbiter is minimum. If there were a way to adaptively and continuously change the data rate of communication, based on the observed instantaneous performance of the link, then the data rate would always be close to the maximum supportable data rate at any given instant, and the resulting received data volume would be much greater.

In the next section we present the summary and current status of ten technology development tasks that are funded by the Communications and Tracking element of the MTP.

4. DESCRIPTION OF THE TASKS

Reprogrammable Transceiver Modem for the Electra Radio

Joseph T. Fieler, Doug Merz, Thomas C. Jedrey,
and Edgar H. Satorius

L-3 Communications Cincinnati Electronics and JPL are collaborating on the design of a Reprogrammable Transceiver Modem Application-Specific Integrated Circuit (ASIC) for future use on Mars. The purpose of this task is to seek size, mass, and power reductions in the Mars proximity link transceivers.

The current state of the art in Mars transceivers is the Electra and Electra-Lite radios. The Electra radio is now flying on the MRO, which launched in August 2005, and the Electra-Lite will fly on the Mars Science Laboratory (MSL), due to launch in 2009. The mass of the BPM of the Electra radio is 1.23 kg. Electra-Lite reduced its BPM mass to 0.85 kg. The goal of this task is to further reduce the mass of the BPM below 0.45 kg, by producing an ASIC based reprogrammable transceiver modem. Mass reduction is a common goal in the space industry, and the reduction of size and mass of the Mars proximity link transceivers is needed to support future small scout-class landers.

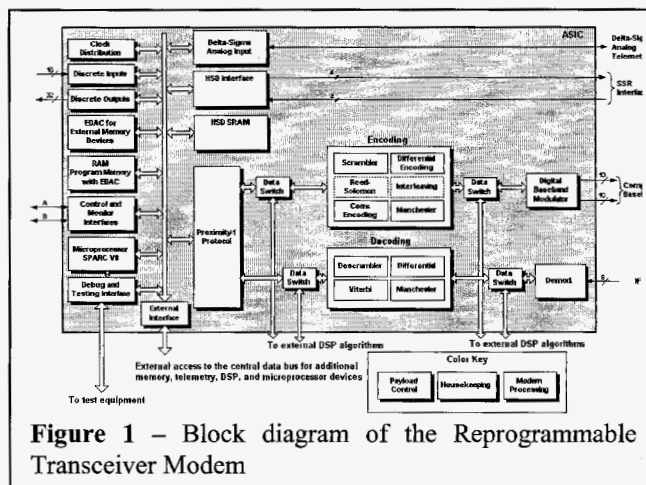


Figure 1 – Block diagram of the Reprogrammable Transceiver Modem

A block diagram of the Reprogrammable Transceiver Modem is shown in Figure 1. The technical approach for achieving the size and mass reduction is to incorporate as much of the previous Electra and Electra-Lite BPM components as possible into a single ASIC package. Modem components that will be integrated into the ASIC include the microprocessor, the Digital Signal Processing (DSP) algorithms, and memory. Software running on the microprocessor shall define most of the functionality of the ASIC. Making the ASIC software defined will give the modem the flexibility and versatility to be used in several missions. The Verilog Hardware Description Language (HDL) from the Electra-Lite transceiver shall form the baseline of the DSP capabilities of the ASIC. The DSP algorithms to be implemented in the ASIC include modulation/demodulation (BPSK and Quadrature Phase

Shift Keying (QPSK)), Forward Error Correction (FEC)/encoding (Reed Solomon, differential, convolutional, Manchester, scrambling randomizer), the Proximity-1 protocol. Memory will be included in the ASIC utilizing either the onboard sea-of-gates, or a multi-chip module. Using the onboard sea-of-gates of the ASIC will limit the total amount of Random Access Memory (RAM) to 8 Mbits. A multi-chip module would significantly increase both the amount and type of RAM, but also the cost of the final product.

Early in 2005 we completed and published a detailed requirements specification document that defines the desired functionality of the ASIC. Currently we are in the phase of developing, building, and testing the modem architecture, selecting ASIC hardware, and producing netlists and test vectors for the ASIC foundry. The following subsystems of the ASIC architecture have already been completed or were previously available: the Scalable Processor ARCHitecture (SPARC) microprocessor, the command and control 1553 interface, the high-speed data interface, the Proximity-1 protocol (both hardware and software), the DSP algorithms (modulation/demodulation), the bus architecture, the debugging and testing interface, the general purpose Input/Output, and the interrupt controller. Over the next year the Verilog HDL code of the Electra-Lite modem will be integrated within the ASIC architecture. The end-product of this task, due at the end of 2006, is a complete HDL description and detailed design documentation of the ASIC, in anticipation of further funding by future missions to fabricate it, flight qualify it and incorporate it into their version of the Electra-Lite radio.

Mars Proximity Microtransceiver

William B. Kuhn, Norman E. Lay, Edwin R. Grigorian and Dan Nobbe

Miniaturized, lightweight, and low-power radio transceivers are needed to support the future exploration of Mars. Such technologies can enable new missions employing multiple scout craft per launch and new vehicle types ranging from aircraft and balloons to networked ground sensors.

Existing radios compatible with the Proximity-1 communication protocols used aboard Mars orbiters measure as large as 5000 cm³, with a mass of up to 5 kg, and consume more than 50 W of power on transmit and 10 W on receive. To fill the need for smaller, lower-power solutions, we are developing a transceiver measuring in the 1 cm³ range and operating at fractions of a Watt of power. It will support transmission rates up to 256 kbps and higher (depending on link parameters) in BPSK or QPSK modulations, and receive command/control instructions at up to 8 kbps. In addition to its low mass/power features, temperature compensated design and radiation tolerance will allow operation outside of large thermally controlled,

shielded enclosures, further reducing the size and mass of the overall scout vehicle.

To achieve our mass, volume and power reduction goals we are employing low-complexity circuit design techniques and conducting system tradeoffs. The miniature transceiver we are designing and building is a two/three chip device that uses a mixed-signal rad-hard Silicon-on-Sapphire

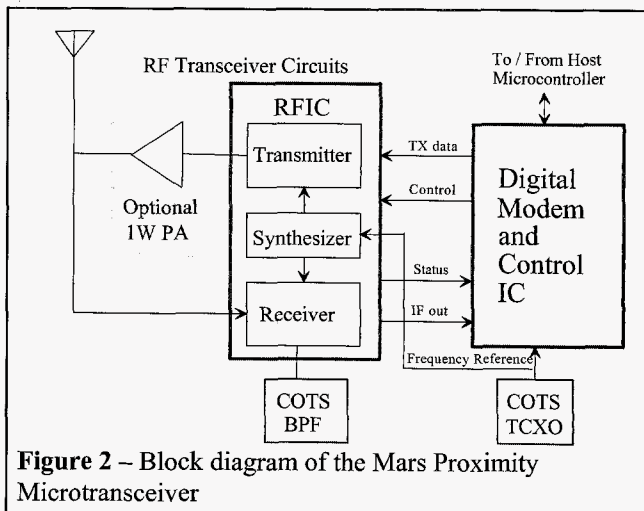


Figure 2 – Block diagram of the Mars Proximity Microtransceiver
 fabrication process. A block diagram of the Mars Proximity Microtransceiver is shown in Figure 2. It employs a Radio Frequency Integrated Circuit (RFIC) die with fully-integrated half-duplex transceiver circuits that trade large-signal performance (not needed in the Mars environment) for lower power consumption on receive. On transmit, it provides either 10 mW or 100 mW RF transmit power output at a good efficiency using high-performance integrated inductors. An optional 1 W power amplifier die can be added for high-volume data return applications. A block diagram of the RFIC is shown in Figure 3.

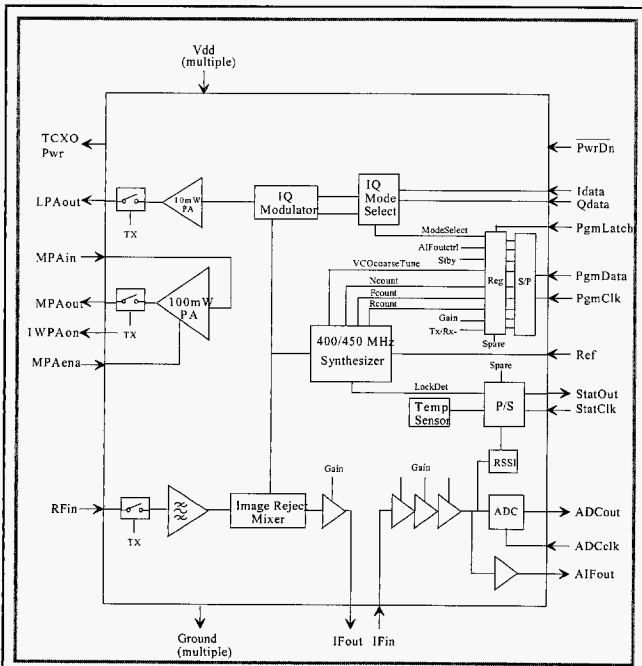


Figure 3 – Block diagram of the Microtransceiver RFIC

A companion digital modem/control die handles transmit data formatting, receive demodulation, bit/frame-synchronization and implements a practical subset of the Proximity-1 protocols. Higher-level protocols such as the go-back-N repeat-request can be provided through the host-system microprocessor and memory subsystems. A block diagram of the Digital Modem and Control IC is shown in Figure 4.

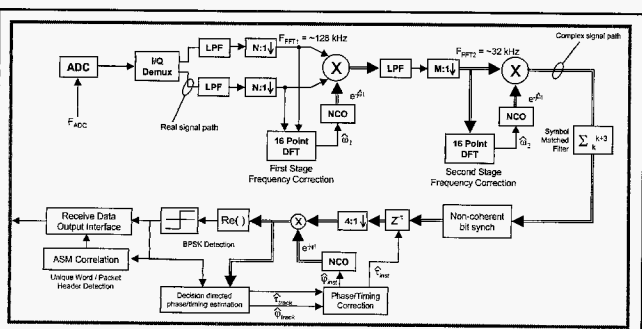


Figure 4 – Block diagram of the Digital Modem and Control IC

In summary, the Mars Proximity Microtransceiver is over two orders of magnitude smaller and lighter than existing transceivers and consumes one to two orders of magnitude less power. To date, the first version of the RFIC receiver circuits have been prototyped in Integrated Circuit form and successfully tested, and the RFIC transmitter circuitry has been submitted to Peregrine Semiconductors, our partner in this task, for fabrication. The digital design is being conducted through a combination of Matlab algorithms and gate-level hardware synthesis, also with good results. Targeted completion for the overall transceiver, including testing at Mars temperatures, is scheduled for mid-2007.

As discussed above, if both ends of the communications link have directive i.e. not low gain) antennas, then moving up in frequency increases the received power as the square of frequency. Both the MERs and the planned 2009 MSL have onboard medium gain X-Band antennas for DTE communication. If we could close the proximity link over the X-Band frequency and communicate from these antennas to a medium or high gain X-Band antenna on the communications relay orbiter we could realize these gains in link performance. Of course, the orbiter X-Band proximity antenna would then have to be steerable (mechanically or electronically) so it can maintain pointing to the lander as the orbiter revolves about Mars. It was planned to equip the Mars Telecom Orbiter (MTO), formerly intended for a 2009 launch, with precisely such a mechanically steerable (gimbaled) X-Band antenna for this purpose. MSL was to have transmitted data to MTO in the X-Band space-to-Earth downlink frequency of 8.4 GHz. Despite the fact that MTO was to have occupied a much higher altitude orbit than Mars Odyssey, resulting in communication ranges exceeding 6000 km, the projected data rate over X-Band was 8 Mbps, much higher than either the MER to Odyssey 256 kbps maximum capability, or the projected MSL to MTO maximum data rate of 64 kbps over the UHF proximity channel. To realize this capability the MTO Electra radio would have to be able to receive the X-Band space-to-Earth downlink frequency of 8.4 GHz. If we wanted a bi-directional X-band proximity link, then the MTO Electra radio would also have to be able to transmit at the Earth-to-space uplink X-band frequency of 7.2 GHz. MTO has since been cancelled due to NASA funding shortfalls, but the concept is valid, and it is thus very desirable for future communications relay orbiters to support X-Band proximity communications.

The objective of this technology development task is to provide the Electra UHF transceiver with a dual UHF and X-Band capability. We are designing, building and testing X-Band Appliqués (two separates modules: one for transmit and one for receive), for the Electra radio, which will downconvert the received X-Band signal to the standard UHF input frequency of the Electra radio, and upconvert the Electra UHF transmitted signal to X-Band. Both the Transmitter Appliqué (upconverter) and the Receiver Appliqué (downconverter) will be settable to either the 7.2 GHz or the 8.4 GHz X-Band frequency to enable fully bi-directional proximity communications. The proposed X-band Appliqués will interface directly with the existing interfaces on the Electra radio. They will allow the Electra radio to operate in pure UHF mode, pure X-Band mode, or mixed UHF/X-Band combinations. Landers equipped with the appropriate Transmitter Appliqué would also be able to communicate DTE.

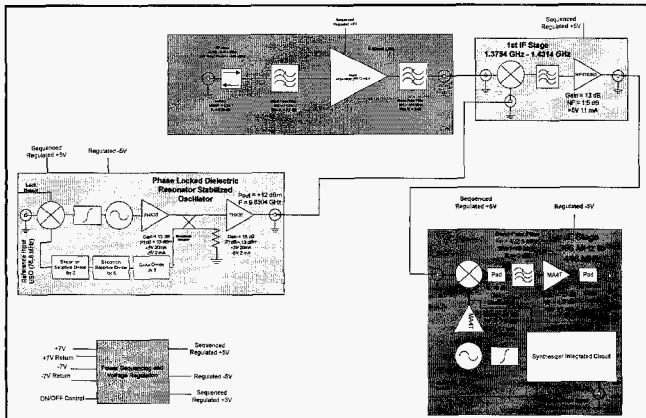


Figure 5 – Block diagram of the Receiver Appliqué

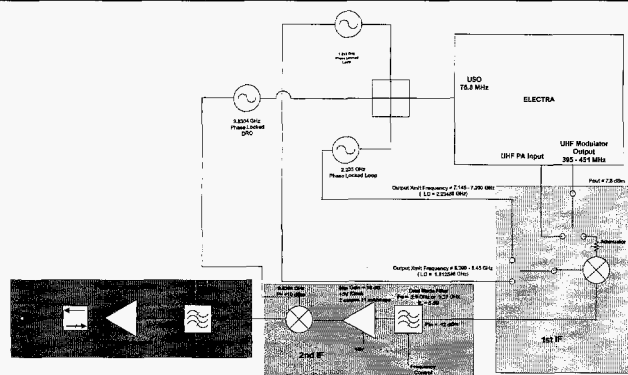


Figure 6 – Block diagram of the Transmitter Appliqué

Block diagrams of the Receiver and Transmitter Appliqués are shown in Figures 5 and 6, respectively. As of October 2005, the theoretical design and simulation of both Receiver and Transmitter Appliqués have been completed and published. The low noise amplifier brass-board has been designed, fabricated and tested, with good results. In order to save mass and volume, a novel approach to X-Band filtering has been utilized, employing a filter topology that is implemented on a hybrid between suspended substrate microstrip and stripline as shown in Figure 7.

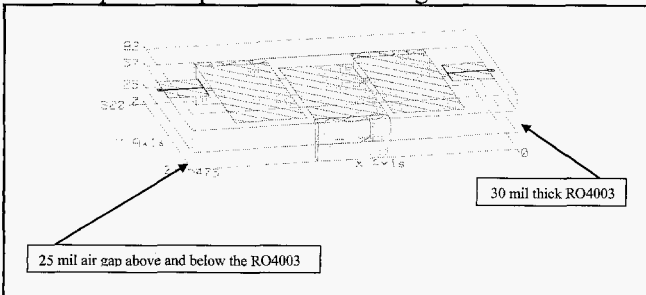


Figure 7 – Reduced size X-Band filter.

We have also designed, fabricated and tested the brass-board of a low phase noise Voltage Controlled Dielectric Resonator Oscillator (VCDRO), a schematic of which is shown in Figure 8. In this novel VCDRO design, the oscillator power is coupled to the output by means of an electric field probe. This ensures that the resonator is lightly loaded, which in turn maintains low output phase noise.

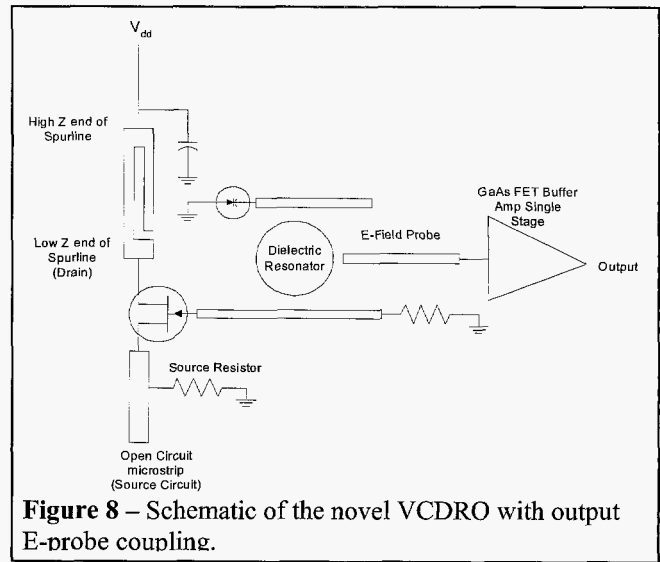


Figure 8 – Schematic of the novel VCDRO with output E-probe coupling.

Next we will fabricate and integrate the downconverter brassboard with the other modules, integrate the VCDRO and the first Intermediate Frequency (IF) section into a common module, test the integrated prototype downconverter, design the RF switch using Electra heritage, design the Solid-State Power Amplifier, fabricate the upconverter brass-board and finally test the upconverter for smooth operation with the Electra radio. This task will deliver operational and tested downconverter and upconverter brassboards versions of the Appliqué in August 2006. These can later be productized and flight qualified on funding from interested missions.

X-Band Agile Beam Transmitter

Jaikrishna Venkatesan and Ronald J. Pogorzelski

As discussed above, moving the communications frequency from UHF to X-Band can dramatically increase the received power at the receiver, everything else being equal, *if* the two communicating elements carry medium or high gain directive antennas. If they do, however, then each must be able to direct the radiated energy of its antenna towards the other, as the two change position with respect to each other.

For low mass, scout-class landers the large mass and volume of a mechanical gimbal that would steer the whole antenna may be prohibitive.

The alternative is to carry a phased array antenna, which can steer the radiated and received beam by adjusting the phase of many small, arrayed, individual radiating elements.

Conventional phased arrays employ phase shifters behind each radiating element to achieve this beam steering. However, the power consumption and design complexity associated with the phase shifters and their control circuitry precludes the use of conventional arrays in low cost and low mass space applications. Another approach to steering the directional high-gain pattern from an array antenna is via coupled oscillators [4-8]. In coupled oscillator phased

arrays, low-power oscillators are employed behind each radiating element in the array, and the adjacent oscillators are coupled together (i.e. energy of adjacent oscillators is purposely coupled into their nearest neighbors, to achieve injection locking of their frequencies). The necessary phase progression along the array that is required for beam steering is generated by simply detuning the resonant frequencies of the end oscillators (perimeter oscillators in a planar array) in opposite directions. Hence, the coupled oscillator beam steering technique avoids the use of phase shifters and their control circuitry as well as the need for a corporate feed design, thus reducing the complexity and cost of the phased array.

Work is currently being conducted at the Jet Propulsion Laboratory to enable low cost, high data-rate in-situ communications in space. An X-band 21-element linear agile beam transmitter employing a coupled oscillator phased array is being designed for high data-rate communications between a Mars rover and a Mars orbiting satellite. In addition to transmitting a signal compatible with the X-band Appliqué of the Electra radio, described above, this 21-element linear coupled oscillator phased array will have the capability of accepting a UHF modulated carrier from the Electra radio and up-converting the modulated signal to X-band for transmission, hence making the array even more attractive for use on future missions.

The concept is illustrated in Figure 9 which shows two arrays mounted on a rover deck providing full sky coverage via two fan beams that can be scanned fore and aft to acquire and track an orbiter.

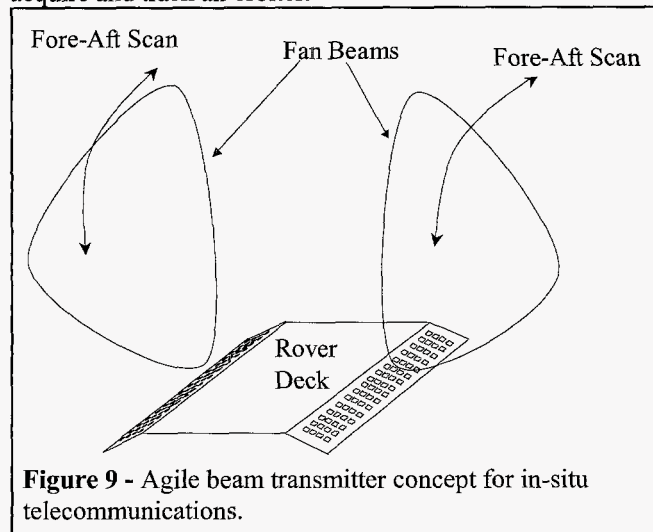


Figure 9 - Agile beam transmitter concept for in-situ telecommunications.

The agile beam transmitter seeks to meet the low cost, high data-rate requirement by realizing a high gain antenna whose directional fan beam is steered using an array of coupled oscillators. The antenna consists of a 21-element microstrip Yagi array that is expected to provide 20 dB of gain.

To validate the radiating aperture concept, a breadboard 3-element microstrip Yagi array employing a dual-offset

aperture-coupled feed has been designed and tested [9, 10]. The antenna concept is shown in Figure 10 illustrating the use of aperture coupling for excitation of the driven element of each Yagi.

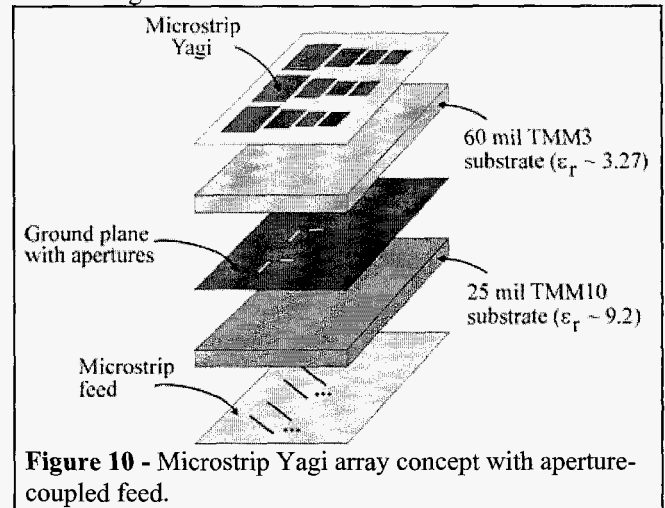


Figure 10 - Microstrip Yagi array concept with aperture-coupled feed.

An aperture-coupled feed was used to provide a low profile, multilayer, tiled array configuration attractive for use on a rover. The fabricated antenna is shown in Figure 11.

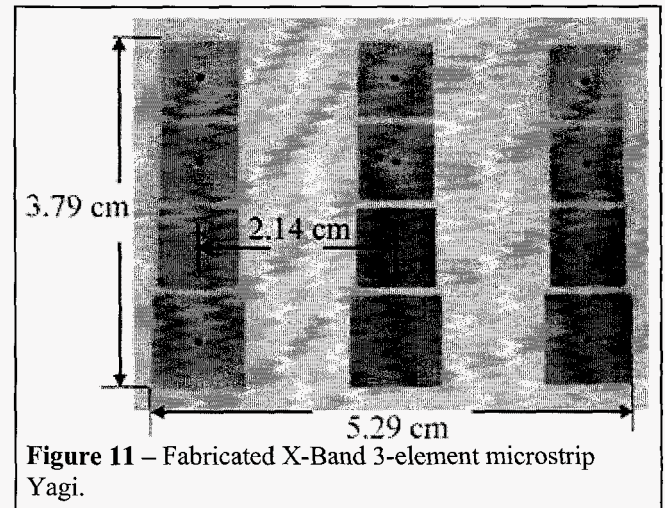


Figure 11 - Fabricated X-Band 3-element microstrip Yagi.

These Yagi elements produce a beam approximately 90 degrees wide along their four element direction. Although the 21-element agile beam transmitter will derive the element excitation from mutually injection locked, coupled oscillators, this array was excited for test purposes using conventional phase shifters to focus the effort on the element performance in the array environment. The measured far field antenna radiation patterns are shown in Figure 12, with the beam "unscanned," and scanned 20 degrees from the normal.

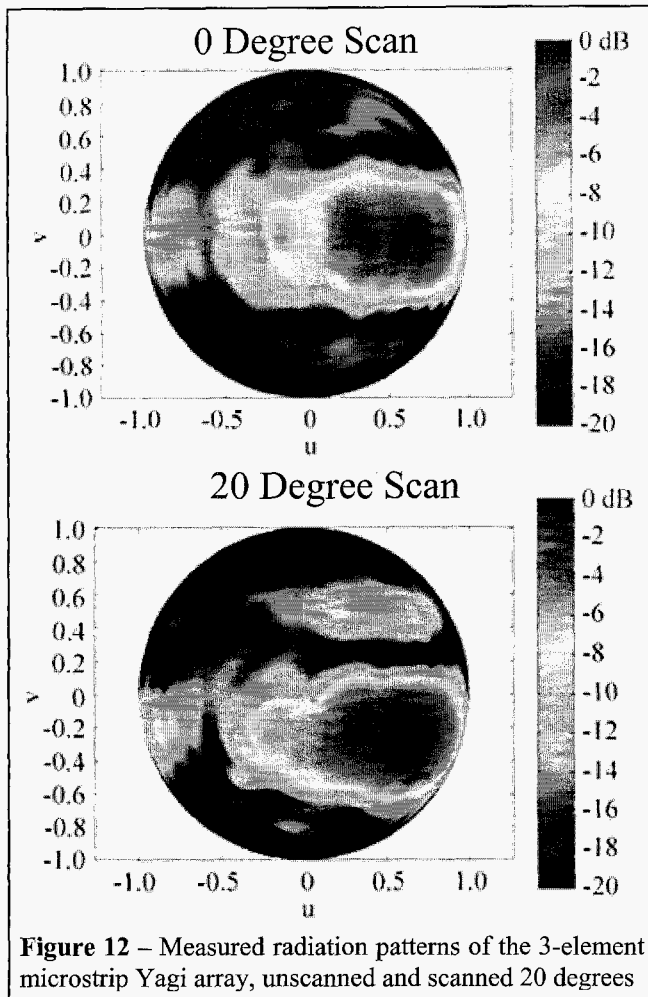


Figure 12 – Measured radiation patterns of the 3-element microstrip Yagi array, unscanned and scanned 20 degrees

Note that these plots are shown in (u,v) space rather than polar coordinates, where $u = \sin\theta \cos\phi$ and $v = \sin\theta \sin\phi$. Also note that because this test array has only three elements, the beamwidth is quite large; i.e., approximately 35 degrees in the three element direction. However, the planned 21-element array is expected to produce a beamwidth of about 5 degrees; that is, the rover agile beam transmitter will have two 20 dB gain fan beams each of a 90 degrees by 5 degrees angular dimension.

In addition to the oscillator array itself, it is necessary to include a diagnostic system that provides real-time assessment of the inter-oscillator phase differences, from which the aperture phase distribution may be determined. This has proven to be an indispensable tool in the initial alignment of the array and in periodic recalibration of the beam steering system during operation. It has further been shown that this system must be built-in as a permanent part of the array, because its removal modifies the array calibration [7]. The oscillator array and phase diagnostic system for this transmitter are currently being designed for separate testing in preparation for the design, fabrication, and test of the full 21-element version planned for completion late in the summer of 2007.

As discussed above, adding a mechanically steered X-Band, medium to high gain antenna to future Mars telecommunications relay orbiters could significantly increase the aggregate data return of future missions that take advantage of the X-Band proximity link.

In either a stowed or deployed configuration, a Mars orbiter, could probably not afford the mass and size of several large antenna apertures. Such an orbiter would be further burdened by the associated mounting hardware and deployment mechanisms of each antenna, all adding significant mass and size. One solution to this problem is to combine two or more antenna apertures into a single unit to reduce mass, complexity and cost, and to free up valuable space on the satellite for other critical sensors and equipment storage. Ball Aerospace & Technologies Corporation (BATC) provides such a solution through its Vitreous® antenna technology. This technology utilizes antennas that are electrically transparent, or Vitreous®, to each other and combines them within the same volume.

Before this technology was available, antennas could be combined utilizing multi-band elements, spatial interlacing of antenna elements, or by stacking or embedding higher frequency elements with lower frequency antennas. These techniques limit the array spacing and layouts because of the physical co-location of the elements and their electrical interactions. The design of all the different frequency antenna arrays is intimately interrelated, and therefore cannot be independently performed to meet system requirements. The stacking technique developed by BATC employs antennas that are electrically transparent to the antennas mounted behind them. Consequently, the so-called Vitreous® arrays can be developed independently, without regard to array spacing or size. Vitreous is an optical term describing the transparent properties of an object. Equivalence between the transmission of light through glass and the transmission of RF energy through metal surfaces exists if the wave properties of light are extended down to RF frequencies.

Vitreous® antennas are made up of Frequency Selective Surfaces (FSSs). By building one antenna out of these surfaces, a second antenna, which operates within the pass band of the FSSs, can be integrated with it. For example, a high frequency antenna can be combined inside a lower frequency Vitreous® antenna. Figure 13 shows a configuration in which low frequency Vitreous® microstrip elements with a solid ground plane are combined with a high frequency planar array. The ground plane is shared by

both the high frequency array and the Vitreous® elements.

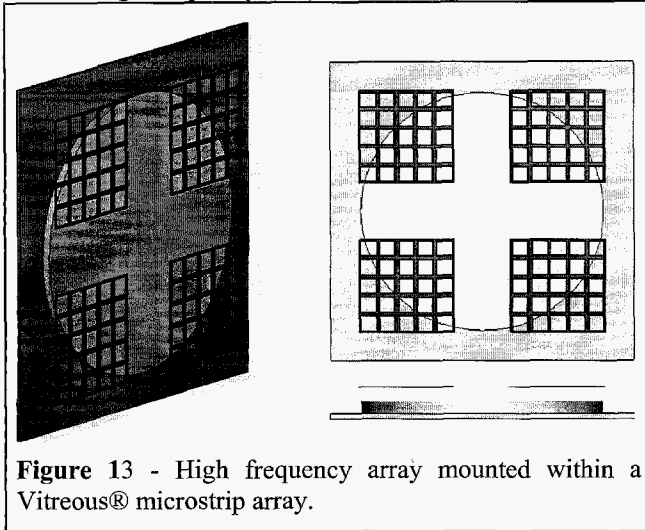


Figure 13 - High frequency array mounted within a Vitreous® microstrip array.

A Vitreous® UHF/X-band antenna array has been developed by BATC for the Jet Propulsion Laboratory (JPL) for future Mars telecommunications relay orbiters. The UHF array consists of nine uniformly fed, non-clocked, square microstrip patch antenna elements. The center patch is Vitreous® with a planar X-band array antenna mounted beneath it. Figure 14 illustrates the relative size and locations. The height of 2" above the ground plane provides sufficient bandwidth for the 390-450 MHz band as well as sufficient spacing from the X-band array to reduce interactions.

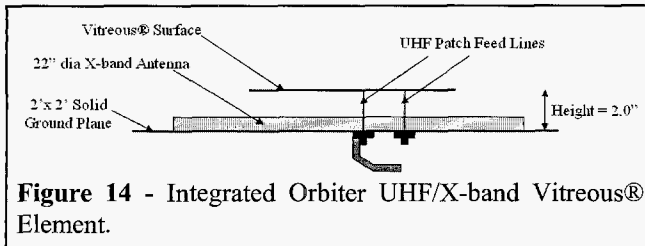


Figure 14 - Integrated Orbiter UHF/X-band Vitreous® Element.

The X-band antenna consists of a dipole array suspended below a polarizer and provides 24 dBic of gain at 7.17 GHz and 27 dBic gain at 8.42 GHz. It is 0.56 m in diameter and 0.02 m thick.

A breadboard antenna was constructed of an aluminum ground plane, a 2-inch foam dielectric spacer, and nine copper-clad G-10 patch elements. The final prototype antenna will consist of a 2" honeycomb dielectric spacer sandwiched between two etched 0.020 inch FR-4 sheets. The two etched FR-4 layers will contain the artwork for all the patch elements and all ground plane circuitry.

A 9-way power divider was designed and fabricated to feed each element of the array corporately. Each output of the power divider was routed to the antenna elements via semi-flexible coaxial cable. Each element of the array was fed with a Lange coupler to provide the proper 0/90 degree phasing and equal power division for Right-Handed

Circular Polarization (RHCP). This configuration was tested on our 75 foot test range (see Figure 15) and exceeded all RF performance goals. It is 1.4 by 1.4 by 0.06 m in size and provides over 15.0 dBic of gain from 390 to 450 MHz, with a peak gain of 16.7 dBic at 430 MHz.

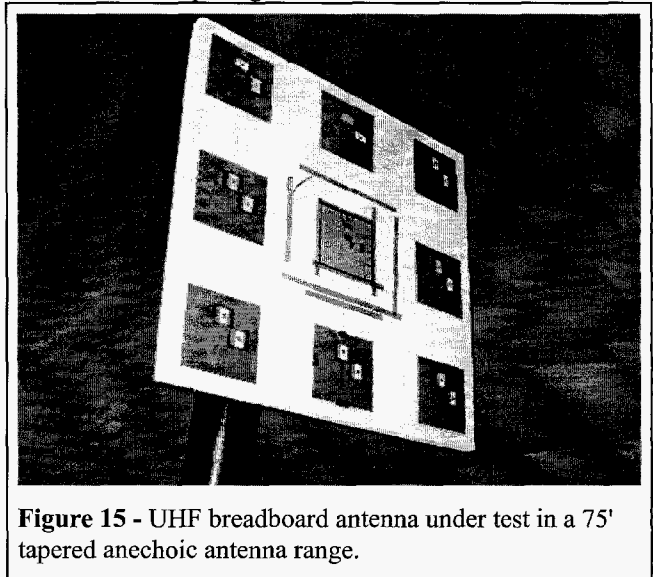


Figure 15 - UHF breadboard antenna under test in a 75' tapered anechoic antenna range.

Figure 16 shows the measured radiation patterns (RHCP and LHCP) at 390 MHz. The sidelobe levels are well below the required 10 dB below the peak gain. The front-to-back ratio remains above 25 dB over the entire back plane.

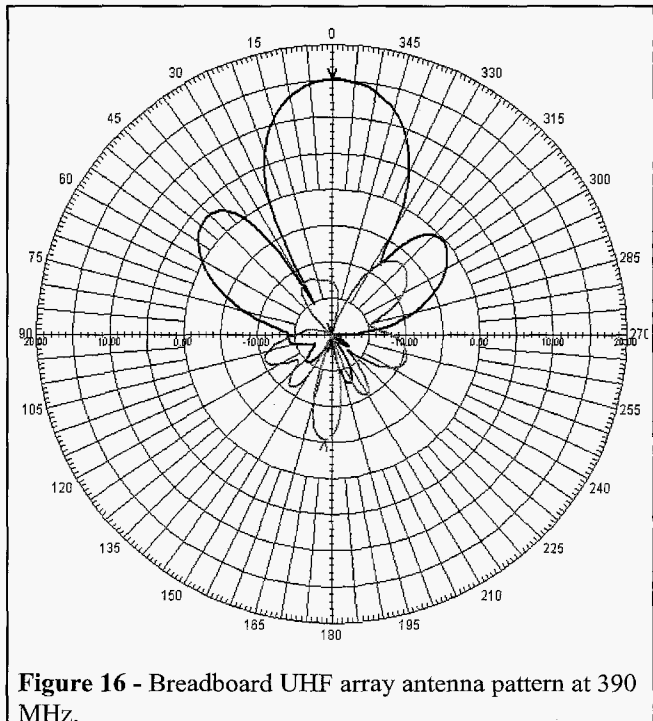


Figure 16 - Breadboard UHF array antenna pattern at 390 MHz.

Work is continuing on this antenna to finalize a mechanical drawing package. This package will be used in building, testing, and delivering a prototype version. The prototype will be electrically and environmentally tested, including

vibration testing, to bring this product to a Technology Readiness Level (TRL) 5.

Large Fresnel Lenses for Optical Ground Receivers

Hamid Hemmati

The two main communication frequencies over which deep space spacecraft downlink data to the Earth today are X-Band (8.4 GHz) and Ka-Band (32 GHz). Because these frequency allocations are spectrally limited by regulatory bodies such as the International Telecommunications Union, we are limited in the data rate we can transmit and return to earth over these bands. At X-Band, with BPSK and/or QPSK modulation plus coding this limit is of the order of a few Mbps. At Ka-Band, where the spectral allocation is 500 MHz wide, this limit is considerably higher, but still under a Gbps order of magnitude. Future Mars exploration, with missions like sample return and even human presence on Mars will require ever higher-data rates, which will eventually hit these limits. Optical communications (laser carrier) with its virtually infinite bandwidth is one solution NASA has been studying for years. Even without bandwidth limitations, considering equation (1), optical links can have immense gains over RF links in received power. The big challenge there of course, is how to point the resulting ultra-narrow beams, a few microradians in angular extent, accurately, from the spacecraft to the earth and vice-versa. After years of study, some hopeful approaches to mitigating this problem have been identified. Another challenge for optical communications is the financial viability of the end-to-end system, given that we would have to recreate from scratch the entire infrastructure that exists for communicating with deep space spacecraft at RF frequencies. One key consideration in this area would be creating affordable optical receiving stations, or telescopes, analogous to the Deep Space Network's large 34 and 70 meter parabolic dish antennas, their RF cousins. This task is an attempt to improve the affordability of such optical receiving stations.

Large diameter (5 meter to greater than 10 meter) Earth-based optical receivers are required to facilitate high data-rate downlink for free-space Optical Communication with space probes. Since photon collection, rather than imaging, is the function of an optical receiver, the required focusing aperture could be less than diffraction-limited in quality. We are investigating the feasibility of utilizing large diameter, custom designed and fabricated Fresnel lenses as the front optical focusing aperture for Earth-based reception of optical communication signals from remote spacecraft. We are investigating optical designs as well as thermal, mechanical, temporal dispersion, and stray-light effects on the performance of these non-diffraction limited photon collection telescopes, sometimes referred to as photon buckets. Some of the attractive features of optical receivers based on Fresnel lenses are:

- With a multi-meter diameter Fresnel lens, it is quite feasible to focus a single wavelength atmospheric-propagated received signal to fit within the 1 mm^2 photon detector that converts the received optical signal to a detected electrical signal (supported by experiments and analysis);
- Fresnel lens replication costs are on the order of a few thousand dollars each, since replication techniques have been perfected for consumer applications. Fabrication time is also quite short compared to that of diffraction limited mirrors and lenses (months versus years).
- They are lightweight (density is less than 1 kg/m^2 compared to about 10 kg/m^2 for light-weighted telescope mirrors).
- They are now manufacturable in large (5-m) diameters with precision diamond turning of a mold and scalable to larger effective diameters through arraying.

Systems engineering issues unique to Fresnel lenses, and techniques to mitigate them include:

Effects of the Atmosphere on the Focal Spot Size: Atmospheric effects (e.g. scintillation and turbulence) increase the blurred focal spot size by a factor of D/r_o , where D is the diameter of the receiving aperture and r_o is the atmospheric coherence length, with typical values of in the 5 to 12 cm range. A 5-m lens, with an r_o of 10 cm, has a D/r_o equal to 50, which corresponds to an atmospheric seeing of 1-2 arcsec. The resulting seeing blurred focal plane circle of about 0.1 mm is small compared to the expected blur spot from the Fresnel lens.

Stray Light Effects: Analysis shows that the largest stray light path (nearly 80% contribution) is from light that suffers a combination of total internal reflection and Fresnel reflections from the surfaces of the Fresnel lens. The other major stray light contributor is scatter from the rounded edges between adjacent facets of the Fresnel lens. Refraction through these edges contributes only 6% to the total stray light. Without further modification of the lens, e.g. anti-reflectance coating, the operational Sun-angle of an optical receiver made of a Fresnel lens will be restricted to angles greater than about 12° of the Sun, which may prove overly restrictive for real-life mission operations.

Thermal Effects: Analysis indicates that significant spherical aberrations can occur with a five Kelvins change in the temperature of a plastic lens. A focal length shift of 0.015% was measured with a 5 K change in temperature. Sunlight pre-filtering is considered an effective mitigation approach.

Effect of Excessive Dust Collection on the Surface: Excessive dust will increase light scatter and attenuation. A

sunlight pre-filter at the dome of the telescope, or frequent cleaning would help to keep dust away from the lens.

Effects of the Lens's Temporal Dispersion on the Communication Signal: Light rays arriving at the focus from the outer zones of the lens are delayed in time relative to those from the central zones. For a 5-m diameter, F/2 refractive Fresnel lens, there is approximately 0.3 m of path length difference (1 nsec delay). For a 10 Mbps link with a 256 Pulse Position Modulation (PPM) format, the slot time is $(8 \times 100 \text{ nsec}) / 256 = 3.1 \text{ ns}$. In this case, a 1 nsec delay is tolerable, but barely so. Mitigating options include: use of slower F numbers for the lens; proper selection of the pulse-width relative to slot width at the transmitter terminal of the link, optical correction, electronic correction, or a combination of these options.

Manufacturing Errors and Tolerancing: Analysis of a 2-m F/1 lens designed for the 1064 nm wavelength indicated that a spot size of 40 micron for 80% encircled energy is theoretically possible. Due to manufacturing errors and tolerances, this level of performance may be difficult to achieve in a manufactured Fresnel lens.

Multiple large diameter (greater than 1-m) commercial off-the-shelf Fresnel lenses and two custom-made lenses (a 2-m four-segmented lens fabricated via replication from a mold, and a 0.6-m directly diamond-turned lens) were purchased and tested. Off-the-shelf lenses produced an unacceptably large spot size of 3 to 5 mm.

Figure 17 shows the preliminary results of measure focal spot size, with the 0.6-m diameter custom designed and fabricated lens.

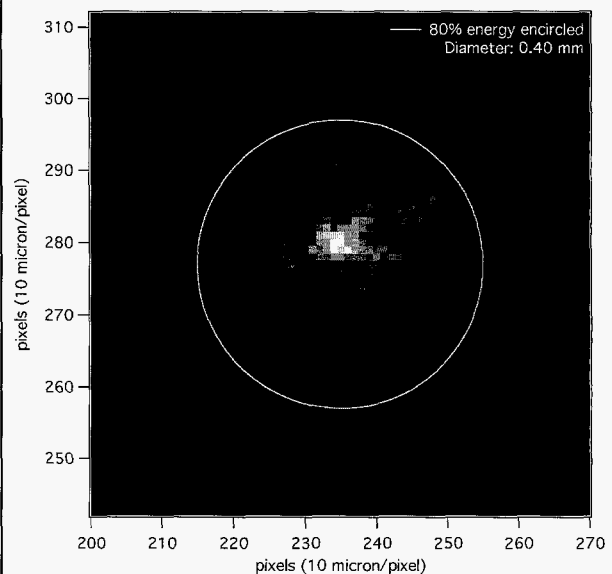
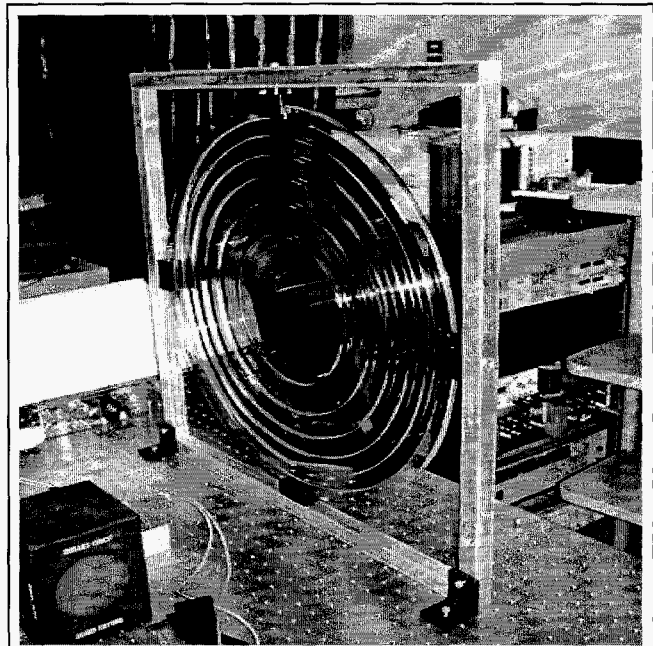


Figure 17 - A 60-cm lens (part of a 2 m diameter lens) diamond turned by Lawrence Livermore National Lab for JPL (top), and the focal spot size of the lens at 1064 nm producing a 0.4-mm spot at 80% encircled energy (bottom).

In 2006 we will complete the 1.5-meter diameter beam collimator, which will allow us to test these large apertures more effectively, we will thoroughly characterize the 0.6-meter lens made by Lawrence Livermore National Lab, and the 2-meter diameter lens made by RHK, Inc. (Japan), and we will pursue creating a custom diamond turned 1.2-m diameter lens (if affordable). Finally we will set-up a lab demonstration optical communication link with a telescope made with the best performing Fresnel lens. The task will culminate in 2007 with a detailed report on Fresnel lenses and the possibilities of their use in large ground optical receiving stations.

Coding System for High Data-Rate Mars Links

Christopher R. Jones, Dariush Divsalar,
Shervin Shambayati and William E. Ryan

The NASA plan for the exploration of Mars calls for a fleet of orbiters and landers to be sent to Mars in the near future. Part of the telecommunications strategy employed for these missions is for the orbiters to relay data from the landers to Earth. This has led to development of the Proximity-1 communications protocol [11], so that communications between orbiters and landers at Mars can be standardized across the lifespan of many potential missions. Unlike direct Mars-to-Earth links, the propagation delay between landers and orbiters is on the order of milliseconds; therefore, these links lend themselves well to the use of an Automatic Repeat Request (ARQ) layer, in addition to the standard FEC codes, to maximize data return (Figure 18).

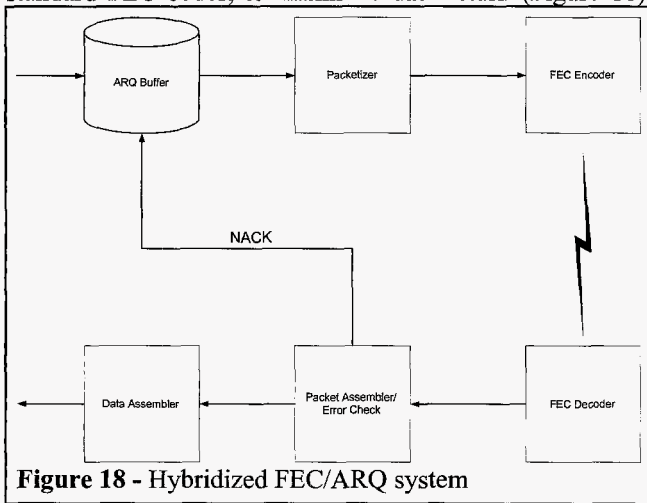


Figure 18 - Hybridized FEC/ARQ system

In order to improve the power efficiency of short haul links at Mars the application of advanced coding techniques to the existing communications infrastructure is in progress. We are proposing the use of a family of capacity achieving LDPC channel codes [12] for FEC, and Go-back-N protocols for ARQ. While other forms of ARQ could yield better overall performance, the extreme simplicity and lack of a need for packet tagging and re-shuffling renders Go-Back-N protocols attractive to implement in radiation hardened, space qualified hardware. The information throughput of the communications link has been optimized, subject to constraints on maximum channel data rate and spacecraft power. This optimization allows selection of the best channel code and packet size at different link path lengths. In the beginning of the optimization procedure the frame error rate of the channel code is expressed as a simple exponential function of the transmitted bit signal-to-noise ratio (E_b/N_0), obtained through curve-fitting. Then the throughput equation for the Go-back-N protocol as a function of the channel code frame error rate is derived. Next, using the equations for the throughput and the frame error rate, the received E_b/N_0 is calculated as a function of the transmitted E_b/N_0 . By minimizing this function, the

throughput of the system is maximized for a given available spacecraft power. In the course of this optimization, we quantify the advantage afforded by a system that supports a set of possible code rates and bandwidths as opposed to a system that uses a single rate at different link communication distances.

The system level combination of FEC and ARQ is often termed hybrid-FEC/ARQ. Rate Compatible Punctured Convolutional Codes (RCPCC) were originally proposed in conjunction with ARQ by Hagenauer et al. [13]. Peric revisited these ideas in the context of a fading satellite communication channel [14]. Recently, rate compatible LDPC codes have been proposed [15] and systems which are able to manage the complexity of the required frame-by-frame FEC/ARQ processing could benefit from these more powerful codes.

The protograph for the AR4A code family [5] for rates 1/2 and higher is shown in Figure 19. This family is the most likely candidate for the proposed system.

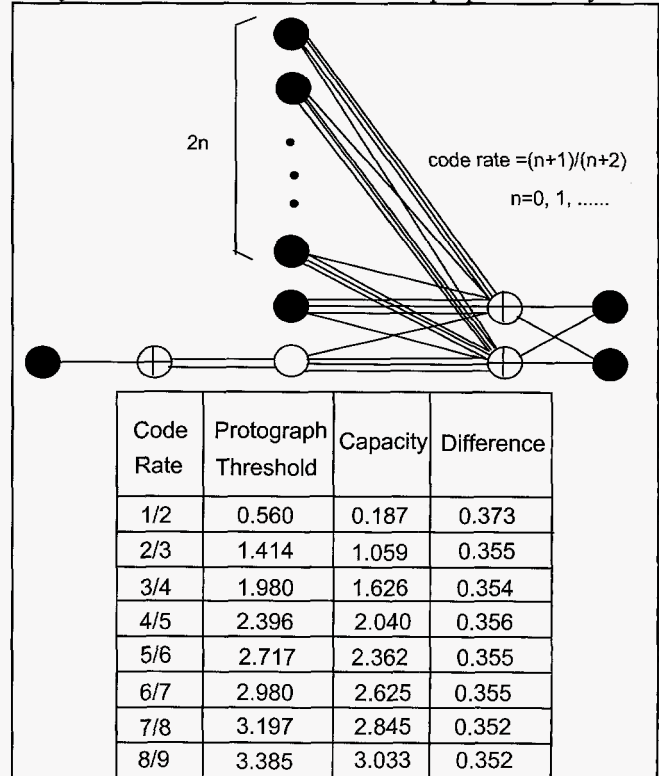


Figure 19 - Protograph of an AR4A LDPC code family.

To realize codes with input length $k=1024$ these protographs were “lifted” using a hybrid of the Progressive Edge Growth (PEG) algorithm [16] and the ACE algorithm [17]. Specifically, PEG is used to expand the initial protograph by a small factor (typically 4 or 8). This initial expansion is done randomly, with the only constraints being that connectivity is dictated by the protograph structure and that graph girth should be maximized greedily per the PEG algorithm. The second expansion employs shifted identity matrices, or circulants, where a given circulant phase is

accepted or rejected based on a criterion known as Approximate Cycle EMD. For instance, the rate-1/6 $k=1024$ code is lifted by a factor of 8 from a protograph that has $k=1$ to form a small code with $k=8$. This small code is then lifted using circulants of size 128 with ACE criteria to achieve a final $k=1024$ block size.

To prove out the LDPC / Go-Back-N ARQ coding scheme that we have invented and enhance the probability of infusion into a future mission, a laboratory demonstration of this proposed scheme, using the Electra radio as a host, is underway. The LDPC encoding and decoding algorithms have been implemented in a Xilinx VirtexII-8000 FPGA. Corresponding control and data signals are interfaced to the Electra radio through a test-port. The Proximity-1 protocol is part of the Electra radio existing functionality. These functions can therefore be leveraged with the exception of packetization, which is different for the LDPC coding scheme from that implemented on Electra for the concatenated convolution/Reed-Solomon coder. The LDPC encoder and decoder are capable of handling code rates extending from 1/3 to 7/8 and block sizes varying between $k=512$ and 4096. Required system throughputs are below 2 Mbps. Both the encoding and decoding functions fit on one FPGA. In addition, sufficient RAM resources remain for I/O buffering of iteratively decoded blocks. Infusion is being conducted in two phases, both of which will be completed by the last quarter of 2006.

Fast and Accurate Electromagnetic (EM) Modeling

Oscar Bruno, Michael C. Haslam, Randy Paffenroth
and Vaughn P. Cable

As discussed above, all recent Mars landers have employed a low gain, low directivity, broad beam UHF antenna, so they can communicate with orbiters that appear to move across the sky without needing to steer their antenna. Although some future landers may migrate to steerable antennas and higher frequencies (X-Band), there will still be smaller, scout-class landers that cannot afford the increased mass, size and power that a steerable antenna entails. Hence, landers will also use UHF low-gain antennas in the future. At UHF the wavelength of the electromagnetic wave is of the order of 70 cm. In order to attain their ideal radiation pattern, low gain antennas require ground planes of the order of a few wavelengths across. It is of course impractical to have an unoccupied circular disk of a few meters about the antenna on the spacecraft deck. Other instruments and spacecraft structures occupy this space and produce reflections, known as multipath, that modify the antenna pattern and produce communications nulls in certain directions [2]. Antenna designers, therefore, cannot design the low gain antenna independently of the spacecraft structure. Hitherto, electromagnetic modeling tools, such as Ansoft Corporations, High-Frequency Structure Simulator, have been used by antenna designers to perform limited simulations of antenna patterns, incorporating some

of the spacecraft geometry around the antenna. Unfortunately these tools are very computationally intensive, and unable to solve the problem of a complete spacecraft (e.g. a rover), using today's computers. Antenna designers are therefore often forced to design, fabricate and measure "mock-ups" of the spacecraft with the antenna integrated. This is an expensive and slow manual process, which involves "cut-and-try" solutions, often lacking analytical foundations.

The object of this task is to create a fully-validated EM simulation infrastructure, with superior capabilities in terms of modeling generality, accuracy and speed, for the prediction of full fidelity near- and far-fields (including multi-path and impedance behavior) in complete multi-material, antenna-spacecraft structures. The tools resulting from this effort will be used to plan, design and optimize UHF proximity links between orbiters and surface landers, and between different surface assets for all Mars missions.

The current state of the art for the solution of integral-equation formulations of Maxwell's equations, the classical Method of Moments, and its accelerated version, the Fast Multipole Method, are intrinsically low accuracy algorithms. JPL projects currently rely on low-fidelity predictions and/or measurements of antenna-spacecraft environment for design, development and mission planning. The numerical methods used require long computing times; e.g. 6 hours on 32 CPUs using approximately 22,000 samples (unknowns) over the spacecraft surface. Caltech's fast and accurate integral-equation solvers, in turn enjoy the following qualities:

- Fast Fourier Transform acceleration, leading to significantly reduced computing times;
- Super-algebraic convergence arising from high-order integration methods;
- Highly accurate high-frequency algorithms;
- Accurate, high-order treatment of singular geometries, including corners, edges and wires;
- High-order representation of the geometries of interest.

These methods have solved, for example, a full Helmholtz problem with 26,000 unknowns in 6.5 hours on 1 CPU, with an error of 0.18%. As part of this effort, these solvers have been extended to the Maxwell case, and for geometries containing singular elements such as corners and edges, with results of equally high quality.

For example, using our new expansion for the thin wire kernel, we have developed a fast solution method for the wire-antenna problem. The method relies on a Chebyshev expansion for the current distribution, which allows the simultaneous treatment of the logarithmic singularity of the

kernel as well as the end point singularity of the solution. Based on the Hallen integral equation formulation of the problem, our code exhibits exponential convergence and, for a wire of 16 wavelengths in length, for instance, our method achieves an accuracy of eight digits with only 80 unknowns and a run time of 2.65 seconds in a single processor AMD XP 2100+ PC.

In addition, we have regularized the Magnetic Field Integral Equation (MFIE) for surfaces containing edges, in which all subtractive cancellations at edges have been resolved by means of a certain two dimensional canonical integral that analytically cancels the leading order term of the current. This approach is quite effective: with just 5766 unknowns, this method provided an accuracy 3.4×10^{-4} for a geometry consisting of two segments of a sphere meeting at a 90 degree angle.

The combined wire and edge solvers have been used to produce the far field of a cylinder with an attached cylindrical monopole antenna, showing excellent agreement with experimental data obtained by the JPL authors.

In 2006 we will document comparison results with measurements of new physical test models, we will develop an accurate EM model of the MER mock-up that was used to characterize UHF antenna patterns and gain in 2003 and we will compare our modeling predictions with archived data from 2003 measurements of the MER mockup. We will document all the above in a final report. This task will culminate in the transfer of our new fast and accurate electromagnetic modeling technology to JPL, for use in the design of future missions.

Adaptive Data-Rates for Electra

Caroline S. Racho, Mandy Wang, Edgar H. Satorius and Thomas C. Jedrey

The goal of the Electra Adaptive Data Rate (ADR) capability is to substantially increase the volume of mission science data sent to a Mars relay orbiter from a lander over the Electra UHF relay link, by varying the communications data rate.

Asymmetries in the low gain antenna patterns of landers, due to multipath reflections from objects on the landers and from surrounding objects in the surface of Mars, create a variable received power profile at the orbiter receiver as the orbiter flies overhead. A polar plot of the radiation pattern of the Spirit MER UHF antenna, with two low elevation passes of Mars Odyssey super-imposed, is shown in Figure 20 (occurred during the morning of Spirit's 21st sol on Mars).

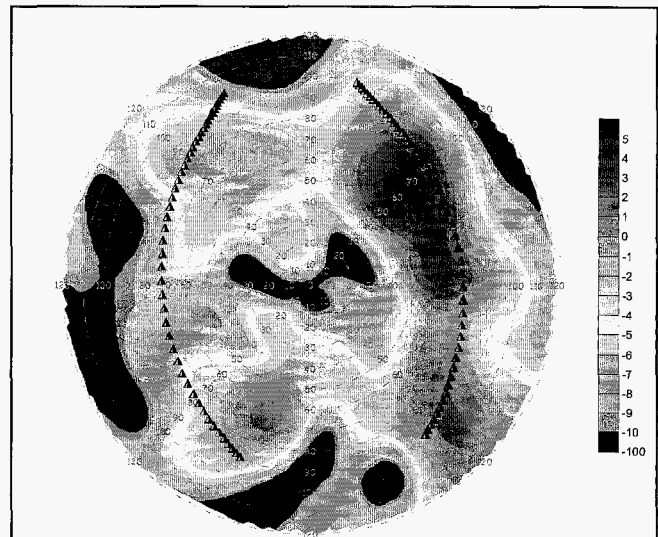


Figure 20 - Two low elevation Odyssey communications passes over the Spirit UHF antenna radiation pattern.

In the right of the two passes the orbiter traverses the good half of the Spirit antenna pattern, and the received power at Odyssey varies primarily with the communications range. In the left of the two passes however, Odyssey goes through a 10 dB null in the Spirit antenna pattern, resulting in a severe reduction of the maximum supportable data rate, as shown in Figure 21.

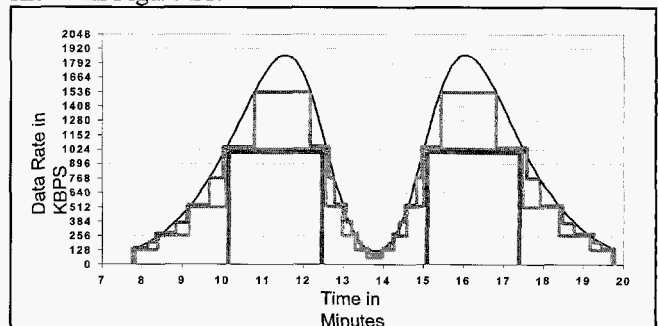


Figure 21 - Maximum supportable data rate of a Spirit-Odyssey pass.

The smooth top curve shows the maximum supportable data rate assuming a continuously variable data rate. The bottom rectangular curve, in two sections, shows the best fixed data rate for this pass. In reality we often choose an even more conservative data rate than that, to account for unpredictable variations in the link performance. The curves between the two show two possible data rate profiles with stepwise data rate changes. The bottom of the two stepwise curves uses data rate steps in factors of two, which is supported by the Electra radio. Since the area under these curves represents the received data volume during this pass, it can be seen from this figure that a great increase in the received data volume could be obtained, if we were able to change the communications data rate during the pass. In fact, a 2003 study conducted at JPL by David Bell and Jon Breen concluded that a 50% increase in returned data volume could be obtained with respect to the best possible fixed

data rate. An even larger increase can be obtained with respect to the more conservative fixed rate that is usually chosen.

In this task we have implemented an Adaptive Data Rate (ADR) capability in the Electra radio. The ADR function is achieved by combining Electra's newly developed ability to monitor the link in real time with the implementation of the Proximity-1 Protocol mechanism of negotiating a data rate change between two Electra radios. To perform end-to-end testing of the new ADR functionality, we have already upgraded the Electra Prototype Test Set, by adding amplitude varying channel hardware, with noise injection capabilities.

Developing an adaptive data rate function for the Electra radio required all hardware and software design modifications to fit into the existing Electra architecture as well as respect its method of operation. The Proximity-1 Protocol developed for proximity space communications defines a procedure which allows adaptive communications. The Requestor of the Proximity Link is allowed to change certain parameters during an open Proximity-1 communication session, one of the important parameters being the communications data rate on the forward and the return link. A block diagram of the implementation selected by the Electra development team for this function is shown in Figure 22.

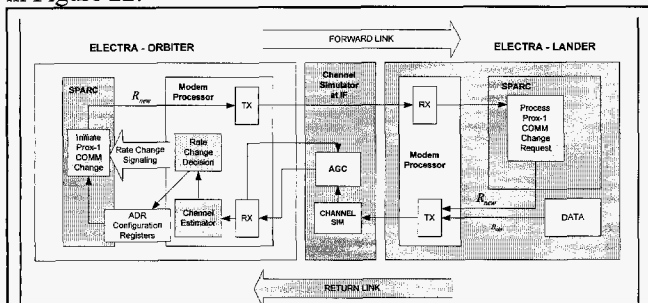


Figure 22 – Block diagram of the Electra Adaptive Data Rates Test Set

The Electra radio on the communications relay orbiter decides and commands the data rate changes. During an established Proximity-1 communications session, the orbiter's Electra continuously monitors the symbol Signal-to-Noise Ratio (SNR) of the return link in real time. A nominal desired operating symbol SNR is stored in a register of the Electra BPM. As the received signal power and channel capacity fluctuate in the simulated example shown in Figure 23, the Rate Change Decision Module in the Modem Processor determines when a data rate change is necessary, resulting in a rate change request which is routed through the Proximity-1 protocol.

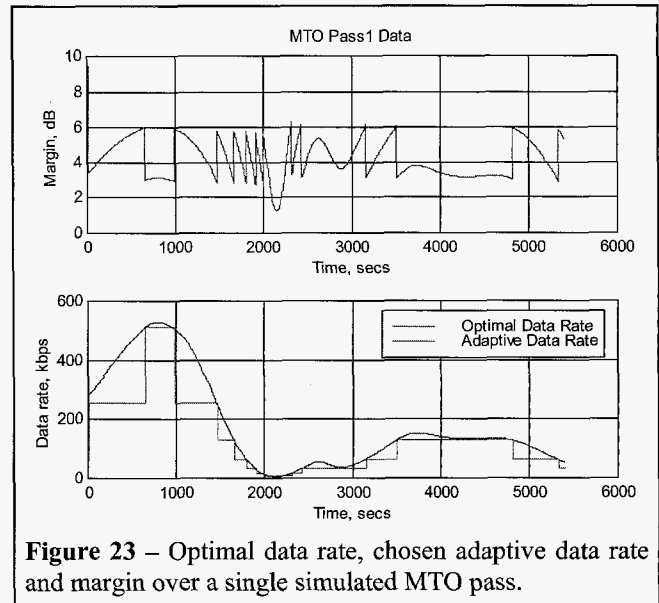


Figure 23 – Optimal data rate, chosen adaptive data rate and margin over a single simulated MTO pass.

In this figure we see the calculated optimal data rate, if it were continuously variable, and the successful stepwise approximation of this data rate effected by the Rate Change Decision Module. Furthermore we see that the average margin remains constant throughout the pass at about 4 dB, without the momentary fluctuations ever reducing it below 1dB. All these parameters are remotely settable.

After the Rate Change Decision Module has decided to change the data rate, the Proximity-1 protocol sends a Proximity-1 Communications Change Request to the lander's Electra radio to decrease or increase its data rate to the next available power-of-two data rate. In cases of precipitous or short duration channel fades the Electra ADR function relies on the Proximity-1 protocol to persist through the outage. For long duration channel outages, the ADR again relies on the Proximity-1 protocol to recover and resume the communications session. The Electra ADR function may be enabled or disabled, by command from the ground.

In order to be able to test the newly implemented Electra ADR functions, a channel simulator and an automatic gain control circuit were added to the existing Electra prototype testbed. Simulated MTO received power levels varied between 20 and 30 dB over a single pass, so we developed a hardware channel emulator that enables us to control the power of the received signal of the Electra radio 70 MHz IF over a range 40 dB. This also required us to add an automatic gain control circuit, emulating the gain control characteristics of the Electra radio engineering and flight units.

In the beginning of the project a floating point simulation of the ADR algorithms was developed for analysis purposes. Upon verification of the approach, a fixed point implementation was implemented for the MRO Electra radio architecture. The implementation of the ADR

function in Electra was separated into two phases: firmware and software. In order to conform to the resources available on the MRO Electra platform, as much as of the ADR function as possible was designed into the firmware. Hence, the Split Symbol Moments SNR Estimator (SSME) as well as the Rate Decision Module were both implemented on Electra's Modem Processor (MP), the flight qualified Virtex 1000 FPGA. Both of these new MP functions have been tested and exist in engineering versions of the MP firmware on the MRO Electra Prototype. The SSME SNR estimator and the Rate Decision Module have been tested in the upgraded MRO Electra equipment rack.

A draft version of the Electra software ADR implementation plan is in place. Under high SNR conditions, preliminary tests of the rate change function embedded within the communication change command of the Proximity-1 protocol have been performed, i.e. the Orbiter Electra can send a Proximity-1 command to the Electra Lander and the Electra Lander effects a data rate change on the return link. This open loop test demonstrates that the Modem Processors can change rates effectively during data transmission when commanded by the SPARC processor to do so.

In order to demonstrate the ADR function with the communication loop closed, i.e., an End-to-End demonstration, the Electra Orbiter software running on the SPARC must be integrated with the Modem Processor ADR firmware. In the next year, the ADR team will integrate the operation of the Proximity-1 rate change software to the signals which are currently generated by the Modem Processor to double or half the current data rates and to detect when the Electra Lander has successfully processed the data rate change command.

At the conclusion of this project, the Electra ADR function will be at a TRL of 5. The development of the firmware and the software will have followed the same development and configuration path as did the MRO flight software and firmware. The documentation will be submitted in the form an Engineering Change Order to the MRO Electra flight system software and firmware. The shortfall in flight readiness will be in that the test cases used to complete the demonstration will not be exhaustive. Such tests would result in the comprehensive fault handling which would be required in flight.

Autonomous Radios for Proximity Links
(Hamkins, Shah, Wang and Stark)

The objective of this task is to design autonomous radio receivers that can autonomously detect the presence and type of arbitrary received communications signals. These autonomous radios will be able to automatically identify the carrier frequency, data rate, modulation type, pulse shape, and presence or absence of a residual carrier, based on properties of the received signal. They will also perform

the conventional functions of determining carrier phase, symbol timing, and signal-to-noise ratio, without the benefit of knowledge of the other parameters mentioned above. This automatic operation will makes it unnecessary to manually configure a receiver for the expected signal type, simplifying complicated reprogramming operations for orbiting radios. This will enable Mars orbiting radios, for example, to receive data from multiple landed assets in rapid succession, without reprogramming the receiver for each lander.

We have demonstrated algorithms that successfully estimate all the above signal parameters, typically using maximum-likelihood approaches [18]. In several cases, determining the performance of the estimators/classifiers by theoretical analysis proved intractable, and algorithm performance was determined and proven by software simulations. To show hardware feasibility, and to advance the technology readiness level of the algorithms, we have begun implementing and demonstrating these algorithms in hardware. The platform selected for the demonstrations is an engineering model of the Electra proximity radio, which is a key element in NASA's plan for the Mars Telecommunications Network [3]. The Electra radio provides navigation, proximity communications, and critical event real-time telemetry capture, and NASA plans to fly Electra on every deep-space mission in the coming decade that utilizes proximity links.

The modulation-type classifier has been successfully implemented and demonstrated on the reprogrammable FPGA contained on the BPM of Electra. The modulation classifier determines, based on the received signal alone, whether BPSK or QPSK was transmitted, and routes the samples to the appropriate demodulator. Hardware tests indicate that with 100 observed symbols and a symbol signal-to-noise ratio of 0 dB, misclassification occurs with probability 1 in 1000, as shown in Figure 24.

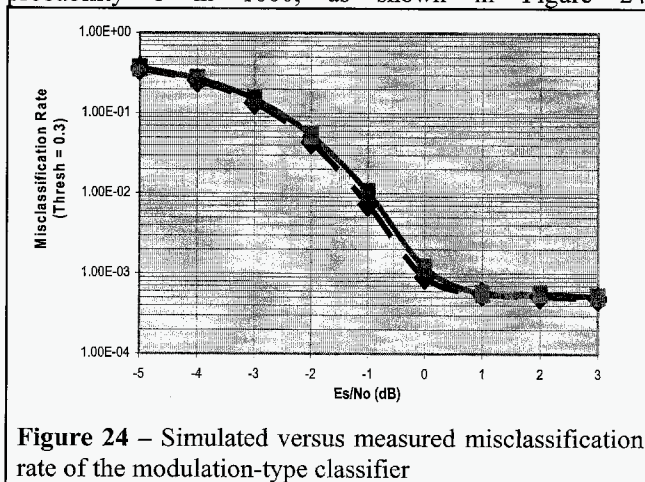


Figure 24 – Simulated versus measured misclassification rate of the modulation-type classifier

In the case of misclassification, the follow-on signal processing would discover the error when bits were not decoded properly, and reclassification would occur. This

classifier was implemented within the spare logic gates of the BPM FPGA, proving that autonomy is practical for NASA missions, using existing radio hardware.

In 2006 we will implement and test fixed-point implementations of the following autonomous signal-identification algorithms:

- Modulation index
- Frequency offset
- Symbol synchronization
- Carrier synchronization
- Joint data-rate/SNR estimator

We will then infuse these algorithms on the Electra radio for testing and verification. Next we will develop techniques for the autonomous optimal configuration of receiving phase-lock loop bandwidth, as a function of the observed data rate. Finally, we will develop autonomous transmitter solutions, employing multiple access asymmetric signaling modulations.

The task will ultimately culminate in 2007 in a set of mature, tested, hardware implementable autonomous radio algorithms ready to be infused in future Mars flight missions.

5. ACKNOWLEDGMENTS

This work was supported by the Mars Technology Program of the Jet Propulsion Laboratory, California Institute of Technology under a contract with the National Aeronautics and Space Administration. Some of the work described in this publication was carried out at the Jet Propulsion Laboratory.

The work of the technology development tasks reported herein was performed by the following individuals, as noted above under the title of each individual task: Vaughn P. Cable, Dariush Divsalar, Edwin R. Grigorian, Jon Hamkins, Hamid Hemmati, Thomas C. Jedrey, Christopher R. Jones, Norman E. Lay, Ronald J. Pogorzelski, Caroline S. Racho, Edgar H. Satorius, Biren N. Shah, Shervin Shambayati, Jaikrishna Venkatesan and Mandy Wang with the Jet Propulsion Laboratory in Pasadena, California; Anthony J. Jensen, with the Ball Aerospace & Technologies Corporation in Westminster, Colorado; Raymond L. Lovestead formerly with the Ball Aerospace & Technologies Corporation in Westminster, Colorado; Oscar Bruno, Michael C. Haslam and Randy Paffenroth with the California Institute of Technology in Pasadena, California; William B. Kuhn with the Kansas State University in Manhattan, Kansas; Joseph T. Fieler, Richard E Hunter Jr.

and Doug Merz with L-3 Communications Cincinnati Electronics in Mason, Ohio; Dan Nobbe with Peregrine Semiconductor in Palatine, Illinois; William E. Ryan with the University of Arizona in Tucson, Arizona; and Wayne E. Stark with the University of Michigan in Ann Arbor, Michigan.

The author of this paper is a Communications Systems Technology Program Manager in the Interplanetary Network Directorate of the Jet Propulsion Laboratory in Pasadena, California. His responsibilities include managing the Communications and Tracking tasks of the MTP.

REFERENCES

- [1] C. D. Edwards Jr. et al., "A Martian Telecommunications Network: UHF Relay Support of the Mars Exploration Rovers by the MGS, Mars Odyssey and Mars Express Orbiters," Proceedings of the IAF Congress, October 2004.
- [2] Andrea Barbieri, Stanley Butman et al., "Development and Flight Performance of CCSDS Proximity-1 on Odyssey and the Mars Exploration Rovers," Proceedings of the 2005 IEEE Aerospace Conference, March 2005.
- [3] Charles D. Edwards Jr., Thomas C. Jedrey et al., "The Electra Proximity Link Payload for Mars Relay Telecommunications and Navigation," IAC-03-Q.3.A.06, Proceedings of the 54th International Astronautical Congress, Bremen, Germany, 29 Sep. – 3 Oct., 2003.
- [4] R. A. York, "Nonlinear analysis of phase relationships in quasi-optical oscillator arrays," IEEE Trans. on Microwave Theory and Tech., MTT-41, 1799-1809, October 1993.
- [5] P. Liao and R. A. York, "A new phase-shifterless beam-scanning technique using arrays of coupled oscillators," IEEE Trans. on Microwave Theory and Tech., MTT-41, 1810-1815, October 1993.
- [6] P. Liao, Electronic beam scanning and millimeter wave power combining using arrays of coupled oscillators, Ph.D. Thesis, University of California Santa Barbara, September 1995.
- [7] R. J. Pogorzelski, "A Five by Five Element Coupled Oscillator Based Phased Array," IEEE Trans. on Antennas and Propagation, AP-53, 1337-1345, April 2005.
- [8] R. Pogorzelski, "A frequency tripled two-dimensional coupled oscillator array," IEEE Trans. on Antennas and Propagation., AP-52, 907-910, March 2004.
- [9] J. Venkatesan, "X-Band Microstrip Yagi Array with Dual Aperture-Coupled Feed", IEEE AP/URSI 2005 International Symposium, Washington, D.C.
- [10] J. Venkatesan, "X-Band Microstrip Yagi Array with Dual-Offset Aperture-Coupled Feed", Microwave and Optical Technology Letters, Accepted for Publication.
- [11] "Proximity-1 Protocol- Data Link Layer," Consultative Committee for Space Data Systems Blue Book 211.0-B-3, <http://public.ccsds.org/documents/211x0b3.pdf>
- [12] R. G. Gallager, Low Density Parity Check Codes. Cambridge, MA: MIT Press, 1963.
- [13] Hagenauer, J., "Rate-compatible punctured convolutional codes (RCPC codes) and their applications," IEEE Transactions on Communications, Volume: 36 , Issue: 4 , April 1988 Pages:389 - 400.
- [14] Peric, M.D., "Performance analysis of the hybrid ARQ/FEC scheme with RCPC codes on fading mobile satellite channel," Telecommunications in Modern Satellite, Cable and Broadcasting Services, 1999. 4th International Conference on , Volume: 1, 13-15 Oct. 1999 Pages:251 - 254 vol.1.
- [15] D. Divsalar, S. Dolinar, C. Jones, "Low-rate LDPC codes with simple protograph structure," To Appear ISIT 2005.
- [16] Arnold D. M., Eleftheriou E., Hu. X. Y., "Progressive edgegrowth Tanner graphs," Proceedings of the 2001 IEEE Global Telecommunications Conference, pp. 995–1001, Vol. 2, San Antonio, TX, 25-29 Nov. 2001.
- [17] Tian T., Jones C., Villasenor J., Wesel R. D., "Characterization and selective avoidance of cycles in irregular LDPC code construction," IEEE Transactions on Communications, Vol. 52, pages 1242–1247, August 2004.
- [18] J. Hamkins and M. Simon, eds., "Autonomous Software-Defined Radio Receivers for Deep Space Applications," John Wiley and Sons, Hoboken, NJ,2006.

BIOGRAPHIES



Dimitrios Antsos is a Communications Systems Technology Program Manager at the Jet Propulsion Laboratory, directing a multi-million dollar spacecraft communications technology development program. Before returning to JPL in April 2003 Dr. Antsos was Chief Operations Officer of Ecliptic Enterprises Corporation, a consulting firm that caters to the commercial aerospace market. Before joining Ecliptic Enterprises Dr. Antsos was Chief Technical Officer of Upstream Systems an international company, currently based in Athens, Greece, providing revolutionary internet-age technologies and services to mass media organizations. Before that Dr. Antsos was R&D manager and senior scientist at Pulsent Corp., a Silicon Valley company performing cutting-edge research in video compression. Prior to that, he was supervisor of the Spacecraft Transponder and Signal Processing group in the Spacecraft

Telecommunications Equipment Section at the Jet Propulsion Laboratory, performing R&D and fabrication of radio telecommunications systems for spacecraft. For five years before 2000, and more recently again in 2004 and 2005, he has also been a lecturer in electrical engineering at the California Institute of Technology. Antsos is the recipient of several NASA certificates of recognition for NASA Tech Brief publications. Antsos holds a bachelor's, a master's and a doctorate in electrical engineering, all from the California Institute of Technology in Pasadena, California.